Title

Athero-inflammatory nanotherapeutics: Ferulic acid-based poly(anhydride-ester) nanoparticles attenuate foam cell formation by regulating macrophage lipogenesis and reactive oxygen species generation

Authors

Chmielowski, Rebecca A
Abdelhamid, Dalia S
Faig, Jonathan J
et al.

Publication Date

2017-07-01

DOI

10.1016/j.actbio.2017.05.029

Peer reviewed

HHS Public Access

Author manuscript

Acta Biomater. Author manuscript; available in PMC 2018 July 15.

Published in final edited form as:

Acta Biomater. 2017 July 15; 57: 85–94. doi:10.1016/j.actbio.2017.05.029.

Athero-Inflammatory Nanotherapeutics: Ferulic Acid-based Poly(anhydride-ester) Nanoparticles Attenuate Foam Cell Formation by Regulating Macrophage Lipogenesis and Reactive Oxygen Species Generation

Rebecca A. Chmielowski[a,*], **Dalia S. Abdelhamid**[c,e,*], **Jonathan J. Faig**[c], **Latrisha K. Petersen**[b], **Carol R. Gardner**[d], **Kathryn E. Uhrich**[c], **Laurie B. Joseph**[d,**], and **Prabhas V. Moghe**[a,b,**]

[a]Department of Chemical and Biochemical Engineering, 98 Brett Rd, Rutgers University, NJ, USA

[b]Department of Biomedical Engineering, 599 Taylor Rd., Rutgers University, NJ, USA

[c]Department of Chemistry and Chemical Biology, 610 Taylor Rd., Rutgers University, NJ, USA

[d]Department of Pharmacology and Toxicology, 160 Frelinghuysen Road, Rutgers University, NJ, USA

[e]Medicinal Chemistry Department, Faculty of Pharmacy, Minia University, Minya, Egypt

Abstract

Enhanced bioactive anti-oxidant formulations are critical for treatment of inflammatory diseases, such as atherosclerosis. A hallmark of early atherosclerosis is the uptake of oxidized low density lipoprotein (oxLDL) by macrophages, which results in foam cell and plaque formation in the arterial wall. The hypolipidemic, anti-inflammatory, and antioxidative properties of polyphenol compounds make them attractive targets for treatment of atherosclerosis. However, high concentrations of antioxidants can reverse their anti-atheroprotective properties and cause oxidative stress within the artery. Here, we designed a new class of nanoparticles with anti-oxidant polymer cores and shells comprised of scavenger receptor targeting amphiphilic macromolecules (AMs). Specifically, we designed ferulic acid-based poly(anhydride-ester) nanoparticles to counteract the uptake of high levels of oxLDL and regulate reactive oxygen species generation (ROS) in human monocyte derived macrophages (HMDMs). Compared to all compositions examined, nanoparticles with core ferulic acid-based polymers linked by diglycolic acid (PFAG) showed the greatest inhibition of oxLDL uptake. At high oxLDL concentrations, the ferulic acid diacids and polymer nanoparticles displayed similar oxLDL uptake. Treatment with the PFAG nanoparticles downregulated the expression of macrophage scavenger receptors, CD-36, MSR-1, and LOX-1 by about 20-50%, one of the causal factors for the decrease in oxLDL uptake. The

**Co-corresponding authors. lbjoseph@pharmacy.rutgers.edu, moghe@rutgers.edu.
*Denotes co-first authors
Contact Author: Prabhas Moghe, Distinguished Professor, Rutgers University, 599 Taylor Road, Piscataway, NJ 08854, USA

PFAG nanoparticle lowered ROS production by HMDMs, which is important for maintaining macrophage growth and prevention of apoptosis. Based on these results, we propose that ferulic acid-based poly(anhydride ester) nanoparticles may offer an integrative strategy for the localized passivation of the early stages of the atheroinflammatory cascade in cardiovascular disease.

Graphical abstract

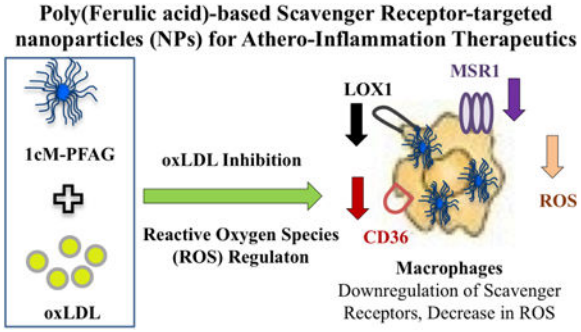

Keywords

atherosclerosis; nanomedicine; ferulic acid; oxidized low density; scavenger receptors

1. Introduction

Cardiovascular disease is the leading cause of death among adults in the United States with medical costs estimated at about $320 billion annually and rising [1]. A major trigger for cardiovascular disease is atherosclerosis, which has a highly complex and chronic inflammatory etiology. A common focal point for the initiation of atherosclerosis is believed to be localized damage to the endothelial lining of the artery, ultimately leading to plaque formation [2-4]. Damage of the endothelium initiates an immune response recruiting monocytes into the subendothelial space where they may differentiate into macrophages [2-4]. As phagocytic cells, macrophages ultimately transform into foam cells after ingestion of oxidized lipids and cholesterol [5]. The subintimal accumulation of foam cells may rupture leading to a cerebrovascular episode [6].

Oxidized low density lipoprotein (oxLDL), a component of foam cells, is a major contributing factor to the escalation of atherosclerosis [7]. Oxidative stress, induced by reactive oxidative and nitrated species, promotes the oxidation of lipids in the blood stream [8]. Oxidized LDL binds to pattern recognition receptors expressed on macrophages, which includes a cluster of differentiation (CD-36), lectin-like oxidized low density lipoprotein receptor (LOX-1), and scavenger receptor A1 (MSR-1) [9]. Uncontrolled macrophage uptake of oxLDL leads to foam cell formation and is a critical trigger for atherosclerosis. Interestingly, there are no current pharmaceutical intervention to directly disrupt foam cell formation. Therefore, there exists a need to develop bioactive formulations to attenuate foam cell formation.

Our laboratories have developed a series of amphiphilic macromolecules (AMs) focused on polymer properties such as charge, stereochemistry, and hydrophobicity, for limiting macrophage uptake of oxLDL [10-12]. Polymer charge is critical for bioactivity since the amphiphilic polymer (denoted as 1cM) containing a carboxylic acid group significantly decreased the uptake of oxLDL in HMDMs compared to an amphiphilic polymer without charge, 0cM [13]. This increase in anionic charge allows 1cM to preferentially interact with macrophage scavenger receptors and competitively bind vis-a-vis oxLDL, which enables further downregulation of the key scavenger receptors, MSR1 and CD36 [14]. To enable long-term stability and activity of the polymers in physiologic microenvironments, the AMs were formulated via flash nanoprecipitation using hydrophobic cores, which result in stable nanoparticles (NPs) [15]. It has also been observed that the 1cM-M12 nanoparticle (comprising 1cM shell and M12 hydrophobic core) is highly efficacious *in vivo* by reducing plaque blockage in the arterial wall [16]. However, the high anionic charge of 1cM and its corresponding hydrophobic analog, M12, can have collateral effects, for example, on the gene expression of inflammatory markers in HMDMs and also modulate the inherent phagocytic activity of macrophages toward bacteria and other foreign substances, such as modified low density lipoprotein [17]. Therefore, we investigated alternative core molecules that could lower the inflammatory state of the macrophages while exhibiting the ability to reduce the macrophage uptake of oxLDL, especially following high levels of atherogenic challenge.

Polyphenol compounds, including vitamin E, have been marketed as atherosclerosis therapeutics due to their hypolipidemic, anti-inflammatory, and antioxidative properties [18-21]. These results have been inconsistent, especially for vitamin E, due to conflicting clinical trial results [22, 23]. The type and dose of anti-oxidant used to assess the progression of atherosclerosis are important factors to consider. Some anti-oxidants will only control the oxidization state of low density lipoprotein while others have been found to contain pro-atherogenic properties, depending on the administered dose [24, 25]. In fact, the delivery of the anti-oxidant is critical since higher concentrations of anti-oxidants can result in establishing localized concentrations of pro-oxidants within the arterial wall, which can inadvertently exacerbate foam cell formation [26]. Therefore, it is essential to design a formulation that can deliver the most efficacious therapeutic dose of the desired anti-oxidant at a gradual, controlled rate while avoiding a burst release.

Ferulic acid is known as a potent natural anti-oxidant, which has been approved as a food additive to prevent lipid peroxidation [27]. Ferulic acid appears to have potential in mitigating atherosclerosis by prevention of smooth muscle cell migration, modulating lipid transport from macrophages, and reducing pro-inflammatory cytokines [28-30]. Pre-treatment with ferulic acid reduced oxLDL uptake by macrophages, which correlated to a reduction in scavenger receptor CD-36 expression while scavenger receptor MSR-1 expression remained unchanged from the control [30]. In addition, pre-treatment with ferulic acid increased expression of ATP-binding cassette transporter A1 (ABCA1), which can facilitate cholesterol efflux and reduce its accumulation in macrophages [28-29].

Ferulic acid is an attractive target for atherosclerosis based on its ability to reduce macrophage lipogenesis. However, the efficacy of ferulic acid may be limited due to

stability, dosing, and delivery to the intended site of action. Our approach for creation of novel ferulic acid nanoparticle formulations contained two main aspects. First, ferulic acid was chemically conjugated within a poly(anhydride-ester) using either an adipic acid or diglycolic acid linker [31, 41]. This approach allowed for protection of the carboxylic acid from decarboxylation, enhanced the total mass of ferulic acid incorporated into the polymer, and allowed for a controlled release of ferulic acid avoiding transient pro-oxidant localized concentrations. The choice of adipic versus diglycolic linker results in different ferulic acid release rates, which allows for fine tuning of formulations for specific atherosclerosis applications. The second aspect involved utilization of the bioactive amphiphilic macromolecule, 1cM. The 1cM is a stabilizing shell for the nanoparticle formulation due to its scavenger receptor targeting and hydrophobic and hydrophilic properties. The hydrophobic carbon arms will allow encapsulation of the ferulic acid-based polymers, while the poly(ethylene glycol) reduces nanoparticle aggregation and subsequent uptake by the reticuloendothelial system (RES) [32]. 1cM has been shown to limit oxLDL uptake in HMDMs by lowering scavenger receptor expression, the strategic role of 1cM as the shell of the nanoparticle will allow enhanced macrophage targeting for delivery of the ferulate-based polymers and diacids [16]. In this paper, we demonstrate the formulation of ferulic acid-based polymers and the diacid intermediates into nanoparticles, which are efficacious as atheroprotection agents against various concentrations of oxidized low density protein (oxLDL) in macrophages. The cellular mechanism of oxLDL inhibition was elucidated by evaluating expression of scavenger receptors, SRA-1, CD36, and LOX-1. In addition, we explore the second key attribute of such newly designed ferulic acid-based nanoparticles, namely their ability to regulate reactive oxygen species (ROS) generation in macrophages as anti-oxidative therapeutics.

2. Materials & Methods

2.1. Reagents, chemicals, and raw materials

All chemicals/materials were purchased from Sigma-Aldrich (Milwaukee, WI) or Fisher Scientific (Pittsburgh, PA) and used as received unless otherwise noted. 18 MΩ·cm resistivity deionized (DI) water was obtained using PicoPure 2 UV Plus (Hydro Service and Supplies - Durham, NC). The following items were purchased from the indicated vendors: Ficoll-Paque Premium and Percoll from GE Healthcare (Pittsburgh, PA), RPMI 1640 from ATCC (Manassas, VA), macrophage colony stimulating factor (M-CSF) from PeproTech (Rocky Hill, NJ), fetal bovine serum (FBS) from Life Technologies (Grand Island, NY), unlabeled oxLDL from Biomedical Technologies Inc. (Stoughton, MA), 3,3′-dioctadecyloxacarbocyanine (DiO) labeled oxLDL from Kalen Biomedical (Montgomery Village, MD), and human buffy coats from either the Blood Center of New Jersey (East Orange, NJ) or New York (New York, NY) blood centers. Flow cytometry (FACS) wash buffer was prepared from phosphate buffered saline (PBS), 0.5 w/v% bovine serum albumin, 0.1 w/v% sodium azide, and 1 v% normal goat serum.

2.2. Amphiphilic macromolecule (AM) and antioxidant molecule synthesis

Macromolecules 1cM and M12 were synthesized as previously detailed and characterized using established techniques including ^{1}H NMR-spectroscopy, gel permeation

chromatography, differential scanning calorimetry, and dynamic light scattering [33-35]. The critical micelle concentration, size, and charge data has been published in the literature [36]. Anti-oxidant molecules were synthesized and characterized as reported previously in the Uhrich laboratory [37]. Figure 1 shows the chemical structures of each anti-oxidant compound.

2.3. Preparation and characterization of nanoparticle formulations

Nanoparticles were fabricated using the flash nanoprecipitation technique as shown in Figure 1 as described previously [15, 38]. Briefly, each shell and core component were dissolved separately in the appropriate solvent and mixed together. The chemical structure of each core component is shown in Supplementary Figure 6. Flash nanoprecipitation was performed by mixing the solvent stream with an aqueous stream containing phosphate buffered solution (PBS) at pH 7.4. The nanoparticles were either dialyzed against PBS using a 6000 MW cutoff ultrafiltration membrane or the solvent was displaced from the solution using vacuum. Nanoparticles were characterized by dynamic light scattering (DLS) using a Malvern-Zetasizer Nano Series DLS detector with a 22 mW He–Ne laser operating at λ 632.8 nm using general purpose resolution mode as previously described [15]. To prepare the sample for zeta potential measurement, each nanoparticle formulation was dialyzed against deionized water using a 3500 molecular weight cutoff ultrafiltration membrane for approximately 24 hours. Approximately 1mL of sample was added into a zeta potential cell and measured using dynamic light scattering. Figure 1 shows the size, polydispersity index (PDI), and zeta potential of each nanoparticle formulation.

2.4. Cell culture of human monocyte derived macrophages (HMDMs)

Peripheral blood derived monocytes (PBMCs) were isolated from human buffy coats by a Ficoll-Paque (1.077 g/cm^3) density gradient followed by a Percoll (1.131 g/cm^3) density gradient as previously described [39]. After both gradient separations, PBMCs were collected and washed with PBS containing 1mM EDTA. PBMCs were plated into FEP teflon-coated cell culture bags at a density of ≥ 8.0×10^7 monocytes per bag. Monocytes were differentiated into macrophages by addition of about 5 to 10 ng/mL recombinant human MCSF and incubated at 37°C in 5% carbon dioxide with media RPMI-1640 supplemented with 2% human serum and 1% P/S for 7 days. After seven days, cell culture bags containing differentiated macrophages were placed on ice for at least 1 hour. The cell suspension was transferred into 50 mL Falcon tubes and centrifuged at 1000 rpm for 10 minutes. Media was removed and cells were resuspended in 20 mL of RPMI-1640, 10% FBS, and 1% P/S. Cells were counted using trypan blue and a hemocytometer. Cells were replated at a density of 150,000 cells/mL and let to rest for at least 1 hour prior to treatment.

2.5. OxLDL uptake and macrophage surface expression by HMDMs

HMDMs were co-incubated with a mixture of labeled and unlabeled DiO oxLDL for a final concentration of either 5 μg/mL or 50 μg/mL and 1×10^{-5} M of nanoparticles in RPMI-1640 with 10% FBS and 1% P/S for 24 hours at 37°C in 5% carbon dioxide. For visualization of MSR-1, unlabeled oxLDL was used in the experiment. Experimental controls included macrophages treated with either medium (basal) or 5 μg/mL or 50 μg/mL of oxLDL. After 24 hours, cells were washed to remove the treatments and 1mL of 10 mM EDTA in PBS pH

7.4 was added to each well. Cells were collected by incubating the plate on ice for up to 15 minutes and removed from the surface of the plate by pipetting and transferred to a flow tube. Each well was washed with 1 mL of FACS buffer, which was also added to the flow tube. Cells were centrifuged at 1000 rpm for 10 minutes at 4°C, supernatant was decanted and cells were resuspended. FACS wash buffer was added to the cells, centrifugated and supernatant decanted. Cells were incubated for 1 hour at 4°C with either PE anti-human MSR1 antibody (clone: U23-56, BD Biosciences), APC anti-human LOX-1 antibody (clone: 15C4, Biolegend) and APC anti-human CD36 antibody (clone: 5-271, Biolegend) or their corresponding isotype control APC mouse IgG2a,κ (clone: MOPC-173, Biolegend) and PE mouse IgG1,κ (clone: MOPC-21, BD Biosciences). Following antibody incubation, the cells were washed twice with FACS wash buffer and then fixed with 1 v% paraformaldehyde in PBS. Cell fluorescence was measured using a Gallios flow cytometer. OxLDL uptake and macrophage surface expression were quantified using the geometric mean fluorescence intensity (MFI) of the intact HMDMs and analyzed using FlowJo software (Treestar). Results are the average of at least three independent experiments with two replicates per experiment. The percentage of oxLDL uptake was calculated using the following formula [40]:

$$\frac{\text{DiO oxLDL MFI of treatment sample}}{\text{DiO oxLDL MFI of oxLDL only control sample}} \times 100 = \text{Percentage of oxLDL uptake} \quad \text{(Eqn 1)}$$

The percentage of macrophage scavenger receptor (SR) expression was calculated using the following formula [40]:

$$\frac{\text{SR MFI of treatment sample}}{\text{SR MFI of oxLDL only control sample}} \times 100 = \text{Percentage of SR expression} \quad \text{(Eqn 2)}$$

2.6. Confocal microscopy

Uptake of oxLDL and expression of CD-36 and MSR-1 were visualized using a SP5 confocal microscope (Leica) with a 40× oil immersion objective. HMDMs were plated in an eight well labtek at a density of 150,000 cells/mL. HMDMs were co-incubated with oxLDL and nanoparticles as described in Section 2.5. HMDMs were washed with PBS pH 7.4 three times and fixed with 4 v% PFA for 20 minutes room temperature. The 4% PFA was removed and cells were incubated with blocking buffer (5 v% goat serum, 0.5 w/v% BSA in PBS pH 7.4) for 15 minutes at room temperature. For CD-36 and MSR-1 expression, HMDMs were treated with 1:50 dilution of the antibodies in blocking buffer overnight at 4°C. Cells were

washed three times with PBS pH 7.4 and then incubated with 1:500 dilution of a goat anti-rabbit secondary IgG antibody tagged with either Alexa Fluor 633 or 647 in blocking buffer for about 30 minutes at room temperature in the dark. Cells were washed three times with PBS pH 7.4 and Hoescht (0.1 μg/mL) was added for 15 minutes. Cells were washed with PBS pH 7.4, covered in foil, and stored at 4°C until imaging.

2.7. Quantification of ferulic acid by reverse phase high performance liquid chromatography (RP-HPLC)

Ferulic acid released from the medium in each nanoparticle treatment with HMDMs was analyzed and quantified using RP-HPLC as described previously [41]. Briefly, an XTerra® RP18 column with a 5 μm pore size and dimensions of 4.6 × 150 mm (Waters, Milford, MA) on a Waters 2695 Separations Module equipped with a Waters 2487 Dual λ Absorbance Detector was utilized for chromatographic separation and detection of ferulic acid. The mobile phase was comprised of 70% of 50 mM KH_2PO_4 with 1 % formic acid at pH 2.5 (Buffer A) and 30% of acetonitrile (Buffer B) run at 1 mL/min at a column temperature of 25°C. Absorbance was monitored at a wavelength of 335 nm and the concentration of ferulic acid in each sample was calculated from a standard curve.

2.8. Anti-oxidant potential by measurement of DPPH and cellular reactive oxygen species (ROS)

Anti-oxidant potential of released ferulic acid was determined using a 2,2-diphenyl-1-picrylhydrazyl (DPPH) radical scavenging assay following previous published methods [42]. In brief, anti-oxidant potential of released ferulic acid was determined by incubating about 100 microliters of the media after a 24 hour treatment of ferulic acid nanoparticles and oxLDL as described above in a DPPH solution (0.024 mg/mL in 3.9 mL methanol). After incubating for 1 hour, the DPPH absorbance change at 517 nm was monitored and compared to a reference (0.1 mL blank – oxLDL solution – in 3.9 mL methanol). DPPH reduction percentage was determined by the equation $[Abs_{t0} – Abs_t]/Abs_{t0} * 100\%$ where Abs_{to} and Abs_t are the reference and sample solution respectively. All studies were conducted in triplicate.

HMDMs were co-incubated with HMDMs were co-incubated with oxLDL and nanoparticles as described in Section 2.5. After 24 hours, each treatment was removed and cells were washed once with PBS pH 7.4 at 37°C. Cells were incubated with 12.5 μM of CellRox Red (Fisher Scientific) at 37°C, 5% carbon dioxide for 30 minutes. The CellRox Red was removed and cells were washed three times with PBS pH 7.4. RPMI-1640, 10% FBS, 1% P/S, 7 g/L HEPES was added to the cells for live imaging at 37°C. OxLDL and ROS fluorescence were visualized using a SP5 confocal microscope (Leica) with a 40× oil immersion objective. ROS levels were quantified by ImageJ and normalized to cell count.

2.9. Statistical analysis

Data presented are from at least three independent experiments ($n \geq 3$) and values are represented as mean ± SEM unless otherwise indicated. Statistical analysis was performed considering $p < 0.05$ to be statistically significant. Statistical significance was determined

using a one-way ANOVA with Tukey's posthoc test for comparisons between multiple treatment groups.

3. Results

3.1 Effect of polymeric antioxidant structure on oxLDL uptake in HMDMs

All nanoparticles with polymer cores ranged from about 160 – 300 nm with a polydispersity index (PDI) of < 0.3, indicating stable and non-aggregated nanoparticles (Figure 1). The 1cM-PFAG and 1cM-PFAA nanoparticles were stable for up to 3 months at 4°C (Supplementary Figure 7A & B), with size changes evident only beyond 3 months at 4°C (Supplementary Figure 7C). The size of the 1cM-FAG acid nanoparticles is within 30 nm after storage up to 3 months at 4°C (Supplementary Figure 7D). The ferulate-based polymer based nanoparticles (i.e., 1cM-PFAG and 1cM-PFAA) will release ferulic acid at a slower rate than their corresponding ferulic diacid nanoparticles (1cM-FAA acid and 1cM-FAG acid) (Supplementary Figure 1A). Therefore, the ferulic diacid nanoparticles will be used to assess the impact of a faster release formulation. The maximum concentration of ferulic acid released into the medium was about 100 μM and occurred with the 1cM-FAG acid nanoparticles (Supplementary Figure 1A). Zeta potential values were uniformly highly negative for all compositions (-24.0 to -27.4 mV), except for 1cM-FAA acid nanoparticles, which were slightly less negative in charge, -18.2mV. The PDI of the nanoparticles with non-polymeric cores, namely ferulic acid diacids (i.e., 1cM-FAG and 1cM-FAA) was 0.3 - 0.4, which indicates these nanoparticles may aggregate over time due to increases in both size and polydispersity. It might be possible to lower the nanoparticle PDI and size by incorporating a lower amount of the ferulic diacids into the nanoparticle assembly. However, for this study, the amount of ferulic acid-based polymer and diacid was held constant between formulations. This reduction in zeta potential for 1cM-FAA acid nanoparticles may also explain the tendency for aggregation of the nanoparticles since the surface charge is reduced.

All of the nanoparticle formulations were statistically significant ($p < 0.01$) for limiting oxLDL transport into HMDMs at an oxLDL concentration of 5 μg/mL (Figure 2A). After treatment with 1cM-PFAG, the oxLDL uptake was about 14% indicating that the 1cM-PFAG displayed the highest bioactivity in HMDMs (Figures 2A & B). In addition, the 1cM-PFAG formulation was statistically significant ($p < 0.05$) for inhibiting oxLDL uptake compared against the 1cM-M12 formulation (Figure 2B). An in-depth analysis of the flow cytometry data revealed the 1cM-PFAG and 1cM-PFAA formulations showed a large reduction of oxLDL uptake for about 25% of macrophages compared to either 1cM-M12 or 1cM-PS (Supplementary Figure 4). 1cM-PFAA, 1cM-FAA, 1cM-FAG, and 1cM-PS displayed similar oxLDL uptake levels ranging from about 20 to 25% (Figure 2A). Confocal images also show lower levels of oxLDL uptake for the ferulic acid nanoparticles compared to the oxLDL control (Figure 2C). It is possible that a small portion of the bioactivity of both the ferulic acid-based polymer and diacid formulations originates from the release of ferulic acid since 100 μM of ferulic acid had an oxLDL uptake of about 70% (Figures 2A & B). The difference in the ferulate-based polymers, PFAA and PFAG, is the adipic versus diglycolic acid linker, which resulted in an additional 5 to 15% of oxLDL inhibition based

on the error bars (Figure 2B). The ferulic acid release profiles and nanoparticle uptake rates of PFAA and PFAG formulations were also substantially different. 1cM-PFAG displayed a slightly higher uptake by HMDMs compared to 1cM-PFAA, which could account for some of the increase in bioactivity (Supplementary Figure 2). In addition, the release of ferulic acid into the media during cell treatment is about 50% for 1cM-PFAG and 20% for 1cM-PFAA (Supplementary Figure 1A). These results suggest that the percentage of ferulic acid released over time is critical for regulating macrophage lipogenesis. The 1cM-PS nanoparticle (with inert core and active shell) showed an oxLDL uptake of about 25% indicating the 1cM shell has a larger contribution for lowering the oxLDL uptake in HMDMs. The oxLDL concentration was increased to 50 μg/mL to determine the effect of the nanoparticle core on oxLDL uptake and scavenger receptor expression.

At an oxLDL concentration of 50 μg/mL, the nanoparticle formulations were found to be statistically significant ($p < 0.01$) for oxLDL uptake compared to the oxLDL and ferulic acid treatments (Figure 2D). The oxLDL transport into macrophages increases by about 6–11% for every nanoparticle formulation (Figures 2D). The oxLDL levels ranged from 25-30% and were similar for the ferulic acid-based polymer and diacid nanoparticles (Figure 2D). Confocal images also show lower levels of oxLDL uptake for the ferulic acid nanoparticles compared to the oxLDL control (Figure 2E). Treatment with either 1cM-PFAG and 1cM-PFAA maintained a subset of macrophages with slightly lower oxLDL uptake (Supplementary Figure 4). The size of this subset population of macrophages was also smaller as indicated by forward light scattering, which also indicates minimal uptake of oxLDL and lower chance of foam cell formation. The oxLDL uptake of 100μM of ferulic acid was minimal at about 90%.

3.2 Effect of polymeric antioxidant structure on scavenger expression in HMDMs

While 1cM-PFAG demonstrates clear efficacy at the reduction of oxLDL uptake by HMDMs, we sought to elucidate the underlying mechanism, by comparing its effects to other control formulations, 1cM-M12 and 1cM-PS nanoparticles. The expression of the following macrophage surface markers were tested by flow cytometry to determine the cellular pathway of oxLDL inhibition: CD-36, MSR-1, and LOX-1. It was notable that 1cM-PFAG displayed a statistically significant ability to down regulate all three of the macrophage receptors. After treatment with 1cM-PFAG and oxLDL at 5 μg/mL, the expression of CD-36 was reduced to about 55% (Figure 3A). The reduction in CD-36 expression directly correlated with a reduction in oxLDL uptake by HMDMs (Supplementary Figure 5). As visualized by confocal, a subset of macrophages contain lower levels of oxLDL but also maintain some surface expression of CD-36 (Figure 3C). 1cM-M12 and 1cM-PFAA nanoparticles also reduce CD-36 expression but to a lesser extent at about 30% (Figures 3A & B). 1cM-M12 has been previously demonstrated to reduce CD-36 expression [40]. After treatment with either 1cM-PFAG or 1cM-PFAA, a subpopulation of macrophages (ie. 20-24% of the cells) displayed a further decrease in CD36 expression as compared to the entire population (Supplementary Figure 5). The CD-36 expression levels of the control formulations, PSPEG-PFAA, PSPEG-PFAG and 1cM-PS, were about 90%, which suggests that the down regulation of CD-36 occurs mainly by macrophage uptake of the nanoparticle by HMDMs and resultant release of the core molecule. When the oxLDL

levels are increased to 50 μg/mL, the CD-36 expression level is at least 90% for all the formulations with exception of 1cM-PFAG (Figure 3D). The CD-36 expression level was about 78% for the 1cM-PFAG nanoparticle, which indicates a 22% increase in CD-36 expression when the oxLDL concentration was increased from 5 to 50 μg/mL.

MSR-1 expression was significantly reduced by 30% after treatment with 1cM-PFAG and 5 μg/mL oxLDL (Figure 4A). An in-depth analysis by flow cytometry shows that the MSR-1 expression is substantially down-regulated in 17% of the macrophage population (Figure 4B). Confocal microscopy images confirm the ability of 1cM-PFAG to down regulate MSR-1 expression compared to the other formulations studied (Figure 4C). From the confocal images and flow cytometry graph, it appears that the majority of macrophages with reduced oxLDL levels after treatment with 1cM-PFAG also have very minimal MSR-1 expression, which contrasts with the trends compared to CD-36 expression. When the oxLDL levels were increased to 50 μg/mL, MSR-1 expression increased to the baseline level even after treatment with 1cM-PFAG (Supplementary Figure 3A). This result indicates that the ability of 1cM-PFAG to down-regulate MSR-1 on HMDMs as a function of oxLDL concentration.

LOX-1 scavenger receptor expression exhibited about a 20% reduction after treatment with 1cM-PFAG and 5 μg/mL of oxLDL (Figure 5A). In contrast, 1cM-M12 and 1cM-PS both displayed a small increase LOX-1 expression. 1cM-PFAG nanoparticles showed a significant reduction of LOX-1 expression compared to 1cM-M12 and 1cM-PS (Figure 5A). About 8% of the macrophage population showed a further reduction of LOX-1 expression after treatment with 1cM-PFAG and 5 μg/mL of oxLDL (Figure 5B). LOX-1 expression ranged from about 90-100% for all formulations when HMDMs were treated with 50 μg/mL of oxLDL (Supplementary Figure 3B). The difference in chemical linker used for the ferulic acid-based polymer (i.e., glycolic versus adipic acid) had a significant effect on the down-regulation of CD-36, MSR-1, and LOX-1 receptors on HMDMs and directly correlated with the ability to reduce oxLDL uptake.

3.3 Effect of polymeric antioxidant structure on regulation of ROS levels in HMDMs

Since oxLDL can activate macrophages and produce high levels of reactive oxygen species (ROS), the effect of each nanoparticle formulation on regulation of ROS was investigated using HMDMs. The ferulic acid polymer and diacid nanoparticles showed the lowest levels of ROS (30-40%) compared to the other formulations with the exception of 1cM-PS (Figure 6A). These results indicate the diglycolic linker did not have a significant impact on the decrease in macrophage ROS levels compared to the polymer with an adipic acid linker. The 1cM-PS nanoparticle also showed lower levels of macrophage ROS at about 37%, which indicated the 1cM shell did not likely elicit substantial increase in macrophage ROS (Figure 6A). However, when the PS core was switched to M12, the ROS levels increased by about 2-fold indicating the M12 core is highly inflammatory (Figure 6A). Furthermore, the nanoparticle core appears to modulate macrophage ROS levels with the ferulic acid polymer and diacid nanoparticles as the most promising formulations for regulating macrophage ROS levels (Figure 6B).

4 Discussion

Long-term sustainable solutions to counteract atherosclerosis will require the chronic administration of pharmacologic molecules that can exhibit efficient bioavailability within the vascular intima where atherosclerotic lesions are concentrated and targeted inhibition of both atherogenesis and pro-oxidative inflammatory processes. To meet the challenge of harnessing the anti-atherogenic properties of antioxidant compounds, more targeted and robust delivery systems are needed to achieve an efficacious dose while limiting localized spikes in pro-oxidants. The emergence of controlled release mechanisms using polymer chemistry coupled with advances in nanotechnology could be one avenue for development of novel, bioactive antioxidant formulations for atherosclerosis applications [43-45]. In this study, we advanced the delivery and formulation of antioxidants through development of ferulic acid-based polymer nanoparticles, which are completely biodegradable and can achieve a sustained and tunable release of ferulic acid to obtain maximum bioactivity for limiting macrophage foam cell formation. By investigation of different ferulic acid intermediate and polymer formulations, we demonstrated the optimal release rate of ferulic acid correlated to a diglycolic linker within the poly(anhydride-ester) backbone for minimizing oxLDL uptake and ROS levels in HMDMs.

The design of ferulic acid nanoparticles was motivated by two factors: hydrophobicity of polymer backbone to control nanoparticle size and ferulic acid release, coupled with the choice of chemical linkers to achieve varying release rates of ferulic acid. Polyanhydrides were chosen for ferulic acid conjugation due to their high surface hydrophobicity, which restricts hydrolytic degradation to the polymer surface and enables a zero order release of ferulic acid [46]. The ferulic acid-based polymers (i.e., PFAG and PFAA) formed stable nanoparticles due to the improved solubility as a polymer over the ferulic acid intermediates (ie. FAG acid and FAA acid). As previously demonstrated, the adipic acid linker releases a small percentage of ferulic acid per day compared to the diglycolic linker when ferulic acid is incorporated into a poly(anhydride-ester) backbone [37]. When ferulic acid is chemically linked using either an adipic or diglycolic acid forming a diacid compound, the release rate is faster than the corresponding polymer moiety (Supplementary Data, Figure 1A). Our findings indicated that when the ferulic acid release rate was increased by the inclusion of the more water-soluble diglycolic linker within the poly(anhydride-ester) (i.e., PFAG), the oxLDL uptake by HMDMs was minimal at 5μg/mL and increased slightly when the oxLDL level was increased to 50 μg/mL. This data suggests 1cM-PFAG may be crucial to prevent the subsequent formation of foam cells.

When macrophages internalize a large amount of oxidized lipoproteins, macrophages will transform into foam cells and become apoptotic [47]. Our results suggest that 1cM-PFAG may decrease plaque necrosis and thrombosis within the arterial wall and thereby preventing macrophage apoptosis and efferocytosis. By reducing oxLDL uptake, macrophages could be potentially preserved, which is critical for the roles that macrophages play in limiting the development and remodeling of plaque and controlling the disease stage of atherosclerosis [48-50]. Together, these results suggest that both the hydrophobicity of the ferulic acid conjugate along with the choice of chemical linker were critical factors in order to formulate bioactive nanoparticles for limiting oxLDL uptake in HMDMs.

We sought to elucidate the nature of cellular mechanisms by which the ferulic acid-based polymer and intermediate nanoparticles modulate oxLDL uptake. We limited our focus on the expression of extracellular scavenger receptors, CD36, MSR1, and LOX1, which predominantly account for uptake of oxLDL by HMDMs [51]. Our results indicated only the 1cM-PFAG nanoparticle was able to significantly downregulate all three HMDM surface scavenger receptors, CD36, MSR1, and LOX-1, at an oxLDL concentration of 5 μg/mL. We hypothesized the downregulation of the above scavenger receptors occurs intracellularly by the release of ferulic acid from the 1cM-PFAG nanoparticle after phagocytosis by HMDMs. When we employed the 1cM-PS formulation, which contains a bioactive shell and non-bioactive polystyrene core, we did not observe any significant downregulation of any of the three scavenger receptors, which validated this hypothesis. When the oxLDL concentration was increased to 50 μg/mL, the ability of 1cM-PFAG to downregulate each cellular receptor was significantly reduced, as expected, which indicated expression of these scavenger receptors is strongly correlated to oxLDL concentration. In addition, since the oxLDL uptake remained low at 30-40%, it is possible that additional scavenger receptors, such as CD163 and SR-B1, could be downregulated by the ferulic acid-based nanoparticles but this mechanism would need further investigation [51]. Furthermore, the ability of ferulic acid nanoparticles to inhibit low density lipoprotein (LDL) oxidation could also be investigated based on previous literature [52].

Recent studies demonstrated a direct correlation of oxLDL uptake in mouse macrophages with an increase in reactive oxygen species (ROS) levels [53, 54]. We hypothesized the primary effect of the ferulic acid nanoparticles is the inhibition of oxLDL receptor expression, which could result in the inihibition of ROS production. Ferulic acid has the potential to scavenge free radicals through its ability to form a resonance stabilized phenoxy radical, which accounts for its antioxidant potential [55, 56]. Our results indicated the ferulic acid-based nanoparticles had a pronounced and statistically significant effect on reducing ROS levels compared to the oxLDL control. Future work could include the investigation of iNOS expression coupled with nitrate/nitrate levels to further understand the inhibition of ROS production. The ability to regulate macrophage ROS has significant implications for atherosclerosis. Reactive oxygen species can play key roles in macrophage polarization along with cell death, proliferation, motility, and phagocytic ability [57]. Taken together this data suggests that 1cM-PFAG reduces the oxLDL uptake and subsequently regulates the generation of ROS by HMDMs, which are two critical aspects for prevention of foam cell formation and apoptosis.

5 Conclusions

Antioxidants have potential as anti-atherogenic agents due to their hypolipidemic and anti-inflammatory properties. However, their bioactivity is limited by the lack of an appropriate delivery system to avoid localized pro-oxidant concentrations. In this study, we advanced the delivery and formulation of antioxidants through development of ferulic acid-based polymer nanoparticles, which are completely biodegradable and can achieve a sustained and tunable release of ferulic acid to obtain maximum bioactivity for limiting macrophage foam cell formation. To our knowledge, this study is the first report demonstrating the ability of ferulic acid polymer nanoparticles to reduce oxLDL uptake and ROS in HMDMs. Furthermore, the

1cM-PFAG nanoparticle downregulated the expression of all three scavenger receptors, CD-36, MSR-1, and LOX-1, which correlated with the reduction in oxLDL uptake by HMDMs. Overall, the formulation of a variety of ferulic acid polymer and intermediate diacid nanoparticles for prevention of macrophage foam cell formation is a major step forward for development of novel, antioxidant formulations for treatment of atherosclerosis.

Supplementary Material

Refer to Web version on PubMed Central for supplementary material.

Acknowledgments

The authors would like to acknowledge the following financial support: National Heart, Lung and Blood Institute at the National Institute of Health (R01HL107913, R21HL93753 - PVM, KEU), the Coulter Foundation for Biomedical Engineering Translational Research Award (PVM), National Institute of Arthritis and Musculoskeletal and Skin Diseases (U54AR055073-LBJ). The authors would also like to acknowledge Theresa Choi and Jessica Cervelli for flow cytometry and confocal microscopy assistance.

References

1. Fleg JL, Forman DE, Berra K, Bittner V, Blumenthal JA, Chen MA, Cheng S, Kitzman DW, Maurer MS, Rich MW, Shen W, Williams MA, Zieman SJ. Secondary prevention of atherosclerotic cardiovascular disease in older adults: a scientific statement from the American Heart Association. Circulation. 2013; 128:2422. [PubMed: 24166575]
2. Libby P. Inflammation in Atherosclerosis. Arterioscler, Thromb, Vasc Biol. 2012; 32:2045. [PubMed: 22895665]
3. Wildgruber, M., Lee, H., Chudnovskiy, A., Yoon, T., Etzrodt, M., Pittet, MJ., Nahrendorf, M., Croce, K., Libby, P., Weissleder, R., Swirski, FK. Recent Advances in Nanotechnology. 1st. Apple Academic Press; 2011. Monocyte subset dynamics in human atherosclerosis.
4. Aviram M. Interaction of oxidized low density lipoprotein with macrophages in atherosclerosis and the antiatherogenicity of antioxidants. Eur J Clin Chem Clin Biochem. 1996; 34:599. [PubMed: 8877334]
5. Moore KJ, Sheedy FJ, Fisher EA. Macrophages in atherosclerosis: a dynamic balance. Nat Rev Immunol. 2013; 13:709. [PubMed: 23995626]
6. Moreno PR, Falk E, Palacios IF, Newell JB, Fuster V, Fallon JT. Macrophage infiltration in acute coronary syndromes. Implications for plaque rupture. Circulation. 1994; 90:775. [PubMed: 8044947]
7. Moore KJ, Tabas I. Macrophages in the Pathogenesis of Atherosclerosis. Cell (Cambridge, MA, U S). 2011; 145:341.
8. Miller YI, Choi S, Wiesner P, Fang L, Harkewicz R, Hartvigsen K, Boullier A, Gonen A, Diehl CJ, Que X, Montano E, Shaw PX, Tsimikas S, Binder CJ, Witztum JL. Oxidation-Specific Epitopes Are Danger-Associated Molecular Patterns Recognized by Pattern Recognition Receptors of Innate Immunity. Circ Res. 2011; 108:235. [PubMed: 21252151]
9. Kzhyshkowska J, Neyen C, Gordon S. Role of macrophage scavenger receptors in atherosclerosis. Immunobiology. 2012; 217:492. [PubMed: 22437077]
10. Chnari E, Lari HB, Tian L, Uhrich KE, Moghe PV. Nanoscale anionic macromolecules for selective retention of low-density lipoproteins. Biomaterials. 2005; 26:3749. [PubMed: 15621265]
11. Faig A, Petersen LK, Moghe PV, Uhrich KE. Impact of Hydrophobic Chain Composition on Amphiphilic Macromolecule Antiatherogenic Bioactivity. Biomacromolecules. 2014; 15:3328. [PubMed: 25070717]
12. Abdelhamid, D., Moghe, PV., Uhrich, KE. Design and synthesis of novel amphiphilic macromolecules for cardiovascular applications. 246th ACS National Meeting & Exposition; Indianapolis, IN, USA. September 8-12; 2013. POLY-189

13. Chnari E, Nikitczuk JS, Uhrich KE, Moghe PV. Nanoscale Anionic Macromolecules Can Inhibit Cellular Uptake of Differentially Oxidized LDL. Biomacromolecules. 2006; 7:597. [PubMed: 16471936]
14. Chnari E, Nikitczuk JS, Wang J, Uhrich KE, Moghe PV. Engineered Polymeric Nanoparticles for Receptor-Targeted Blockage of Oxidized Low Density Lipoprotein Uptake and Atherogenesis in Macrophages. Biomacromolecules. 2006; 7:1796. [PubMed: 16768400]
15. York AW, Zablocki KR, Lewis DR, Gu L, Uhrich KE, Prud'homme RK, Moghe PV. Kinetically Assembled Nanoparticles of Bioactive Macromolecules Exhibit Enhanced Stability and Cell-Targeted Biological Efficacy. Adv Mater (Weinheim, Ger). 2012; 24:733.
16. Lewis DR, Petersen LK, York AW, Zablocki KR, Joseph LB, Kholodovych V, Prud'homme RK, Uhrich KE, Moghe PV. Sugar-based amphiphilic nanoparticles arrest atherosclerosis in vivo. Proc Natl Acad Sci U S A. 2015; 112:2693. [PubMed: 25691739]
17. Lewis DR, Moghe PV, Petersen LK, York AW, Ahuja S, Chae H, Joseph LB, Rahimi S, Haser PB, Uhrich KE. Nanotherapeutics for inhibition of atherogenesis and modulation of inflammation in atherosclerotic plaques. Cardiovasc Res. 2016; 109:283. [PubMed: 26472131]
18. Auger C, Rouanet J, Vanderlinde R, Bornet A, Decorde K, Lequeux N, Cristol J, Teissedre P. Polyphenols-enriched Chardonnay white wine and sparkling Pinot Noir red wine identically prevent early atherosclerosis in hamsters. J Agric Food Chem. 2005; 53:9823. [PubMed: 16332138]
19. Opie LH. New developments in cardiovascular drugs: vitamin E and antioxidants - an informal and personal viewpoint. Cardiovasc Drugs Ther. 1997; 11:719. [PubMed: 9512866]
20. Rao GHR, Parthasarathy S. Antioxidants, atherosclerosis and thrombosis. Prostaglandins, Leukotrienes Essent. Fatty Acids. 1996; 54:155.
21. Illingworth DR. The potential role of antioxidants in the prevention of atherosclerosis. J Nutr Sci Vitaminol. 1993; 39:S43. [PubMed: 8164066]
22. Munteanu A, Zingg JM, Azzi A. Anti-atherosclerotic effects of vitamin E - myth or reality? J Cell Mol Med. 2004; 8:59. [PubMed: 15090261]
23. Tardif JC. Antioxidants: the good, the bad and the ugly. Can J Cardiol. 2006; 22(B):61B.
24. Catapano AL, Maggi FM, Tragni E. Low density lipoprotein oxidation, antioxidants, and atherosclerosis. Curr Opin Cardiol. 2000; 15:355. [PubMed: 11128189]
25. Stocker R. The ambivalence of vitamin E in atherogenesis. Trends Biochem Sci. 1999; 24:219. [PubMed: 10366846]
26. Hood E, Simone E, Wattamwar P, Dziubla T, Muzykantov V. Nanocarriers for vascular delivery of antioxidants. Nanomedicine (London, U K). 2011; 6:1257.
27. Srinivasan M, Sudheer AR, Menon VP. Ferulic acid: therapeutic potential through its antioxidant property. J Clin Biochem Nutr. 2007; 40:92. [PubMed: 18188410]
28. Hou YZ, Yang J, Zhao GR, Yuan YJ. Ferulic acid inhibits vascular smooth muscle cell proliferation induced by angiotensin II. Eur J Pharmacol. 2004; 499:85. [PubMed: 15363954]
29. Chen FX, Wang LK. Effect of ferulic acid on cholesterol efflux in macrophage foam cell formation and potential mechanism. Zhongguo Zhongyao Zazhi. 2015; 40:533. [PubMed: 26084183]
30. Xie C, Kang J, Chen JR, Nagarajan S, Badger TM, Wu X. Phenolic Acids Are in Vivo Atheroprotective Compounds Appearing in the Serum of Rats after Blueberry Consumption. J Agric Food Chem. 2011; 59:10381. [PubMed: 21866950]
31. Ouimet MA, Faig JJ, Yu W, Uhrich KE. Ferulic Acid-Based Polymers with Glycol Functionality as a Versatile Platform for Topical Applications. Biomacromolecules. 2015; 16:2911. [PubMed: 26258440]
32. Jokerst JV, Lobovkina T, Zare RN, Gambhir SS. Nanoparticle PEGylation for imaging and therapy. Nanomedicine (London, U K). 2011; 6:715.
33. Djordjevic J, del Rosario LS, Wang J, Uhrich KE. Amphiphilic scorpion-like macromolecules as micellar nanocarriers. J Bioact Compat Polym. 2008; 23:532.
34. Iverson NM, Sparks SM, Demirdirek B, Uhrich KE, Moghe PV. Controllable inhibition of cellular uptake of oxidized low-density lipoprotein: structure-function relationships for nanoscale amphiphilic polymers. Acta Biomater. 2010; 6:3081. [PubMed: 20170758]

35. Tian L, Yam L, Zhou N, Tat H, Uhrich KE. Amphiphilic Scorpion-like Macromolecules: Design, Synthesis, and Characterization. Macromolecules. 2004; 37:538.
36. Wang J, Plourde NM, Iverson N, Moghe PV, Uhrich KE. Nanoscale amphiphilic macromolecules as lipoprotein inhibitors: the role of charge and architecture. Int J Nanomed. 2007; 2:697.
37. Ouimet, MA. Rutgers University Thesis. 2013. Design, synthesis, and fabrication of biodegradable, bioactive-based polymers for controlled release applications.
38. Chan JW, Lewis DR, Petersen LK, Moghe PV, Uhrich KE. Amphiphilic macromolecule nanoassemblies suppress smooth muscle cell proliferation and platelet adhesion. Biomaterials. 2016; 84:219. [PubMed: 26828686]
39. Menck K, Behme D, Pantke M, Reiling N, Binder C, Pukrop T, Klemm F. Isolation of human monocytes by double gradient centrifugation and their differentiation to macrophages in teflon-coated cell culture bags. J Visualized Exp. 2014; 91:e51554/1–e51554/10.
40. Petersen LK, York AW, Lewis DR, Ahuja S, Uhrich KE, Prud'homme RK, Moghe PV. Amphiphilic Nanoparticles Repress Macrophage Atherogenesis: Novel Core/Shell Designs for Scavenger Receptor Targeting and Down-Regulation. Mol Pharmaceutics. 2014; 11:2815.
41. Ouimet MA, Faig JJ, Yu W, Uhrich KE. Ferulic Acid-Based Polymers with Glycol Functionality as a Versatile Platform for Topical Applications. Biomacromolecules. 2015; 16:2911. [PubMed: 26258440]
42. Scherer R, Godoy HT. Antioxidant activity index (AAI) by the 2,2-diphenyl-1-picrylhydrazyl method. Food Chem. 2008; 112:654.
43. Stebbins ND, Faig JJ, Yu W, Guliyev R, Uhrich KE. Polyactives: controlled and sustained bioactive release via hydrolytic degradation. Biomater Sci. 2015; 3:1171. [PubMed: 26222033]
44. Dalmolin LF, Khalil NM, Mainardes RM. Delivery of vanillin by poly(lactic-acid) nanoparticles: Development, characterization and in vitro evaluation of antioxidant activity. Mater Sci Eng, C. 2016; 62:1.
45. Kim S, Park H, Song Y, Hong D, Kim O, Jo E, Khang G, Lee D. Reduction of oxidative stress by p-hydroxybenzyl alcohol-containing biodegradable polyoxalate nanoparticulate antioxidant. Biomaterials. 2011; 32:3021. [PubMed: 21292318]
46. Anon. Excipient Development for Pharmaceutical, Biotechnology, and Drug Delivery Systems. Ashok Katdare and Mahesh V. Chaubal. Pharm Dev Technol. 2007; 12:109.
47. Seimon T, Tabas I. Mechanisms and consequences of macrophage apoptosis in atherosclerosis. J Lipid Res. 2009; (1):S382. [PubMed: 18953058]
48. Botham KM, Wheeler-Jones CPD. Postprandial lipoproteins and the molecular regulation of vascular homeostasis. Progress in Lipid Research. 2013; 52:446. [PubMed: 23774609]
49. Feig JE, Parathath S, Rong JX, Mick SL, Vengrenyuk Y, Grauer L, Young SG, Fisher EA. Reversal of hyperlipidemia with a genetic switch favorably affects the content and inflammatory state of macrophages in atherosclerotic plaques. Circulation. 2011; 123:989. [PubMed: 21339485]
50. Feig JE, Rong JX, Shamir R, Sanson M, Vengrenyuk Y, Liu J, Rayner K, Moore K, Garabedian M, Fisher EA. HDL promotes rapid atherosclerosis regression in mice and alters inflammatory properties of plaque monocyte-derived cells. Proc Natl Acad Sci. 2011; 108:7166. [PubMed: 21482781]
51. Greaves DR, Gordon S. Thematic review series: the immune system and atherogenesis. Recent insights into the biology of macrophage scavenger receptors. J Lipid Res. 2005; 46:11. [PubMed: 15548472]
52. Bourne LC, Rice-Evans CA. The effect of the phenolic antioxidant ferulic acid on the oxidation of low density lipoprotein depends on the pro-oxidant used. Free Radic Res. 1997; 27:337. [PubMed: 9350437]
53. Lee SJ, Quach CHT, Jung KH, Paik JY, Lee JH, Park JW, Lee KH. Oxidized low-density lipoprotein stimulates macrophage 18F-FDG uptake via hypoxia-inducible factor-1Î± activation through Nox2-dependent reactive oxygen species generation. J Nucl Med. 2014; 55:1699. [PubMed: 25214643]
54. Bae YS, Lee JH, Choi SH, Kim S, Almazan F, Witztum JL, Miller YI. Macrophages Generate Reactive Oxygen Species in Response to Minimally Oxidized Low-Density Lipoprotein. Circ Res. 2009; 104:210. [PubMed: 19096031]

55. Yanai N, Shiotani S, Hagiwara S, Nabetani H, Nakajima M. Antioxidant combination inhibits reactive oxygen species mediated damage. Biosci, Biotechnol, Biochem. 2008; 72:3100. [PubMed: 19060409]

56. Graf E. Antioxidant potential of ferulic acid. Free Radical Biol Med. 1992; 13:435. [PubMed: 1398220]

57. Tan HY, Wang N, Li S, Hong M, Wang X, Feng Y. The Reactive Oxygen Species in Macrophage Polarization: Reflecting Its Dual Role in Progression and Treatment of Human Diseases. Oxid Med Cell Longev. 2016; 2016:2795090. [PubMed: 27143992]

Statement of Significance

Future development of anti-oxidant formulations for atherosclerosis applications is essential to deliver an efficacious dose while limiting localized concentrations of pro-oxidants. In this study, we illustrate the potential of degradable ferulic acid-based polymer nanoparticles to control macrophage foam cell formation by significantly reducing oxLDL uptake through downregulation of scavenger receptors, CD-36, MSR-1, and LOX-1. Another critical finding is the ability of the degradable ferulate-based polymer nanoparticles to lower macrophage reactive oxygen species (ROS) levels, a precursor to apoptosis and plaque escalation. The degradable ferulic acid-based polymer nanoparticles hold significant promise as a means to alter the treatment and progression of atherosclerosis.

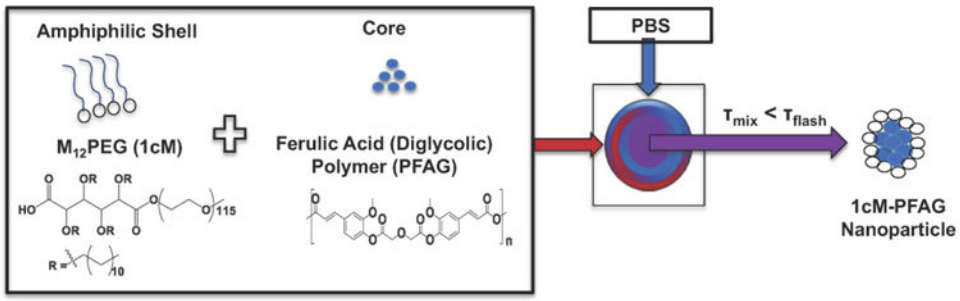

Shell Material	Core Material	Nanoparticle	$Z_{average}$ (nm)	Polydispersity Index (PDI)	Zeta Potential (mV)
1cM (M12P5)	M12		168 ± 9	0.233 ± 0.055	-24.0
	Polystyrene (PS)		264 ± 34	0.151 ± 0.006	-26.4
	PFAG		215 ± 31	0.252 ± 0.056	-25.5
	PFAA		236 ± 20	0.140 ± 0.009	-27.4
PS-PEG	PS		150 ± 17	0.212 ± 0.071	N/A
	PFAG		180 ± 39	0.286 ± 0.072	N/A
	PFAA		205 ± 21	0.242 ± 0.053	N/A

Figure 1. Nanoparticle Formulation & Results Summary

Top: Description of the flash nanoprecipitation process for the formulation of 1cM-PFAG nanoparticles. *Bottom:* Table with size, PDI, and zeta potential results for each nanoparticle formulation.

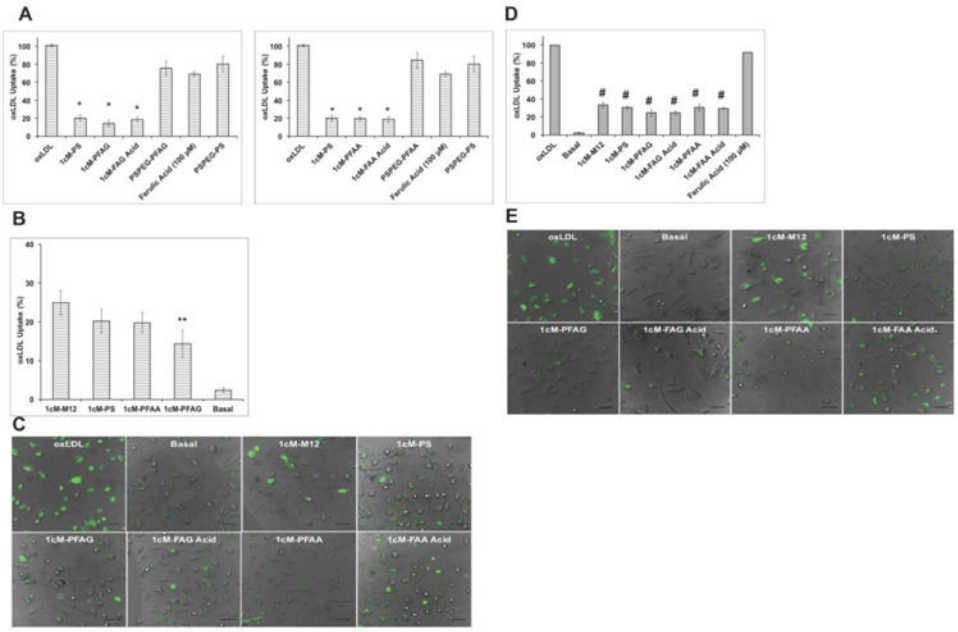

Figure 2. Effect of Ferulic Acid-based Poly(anhydride-ester) Nanoparticles on oxLDL uptake in HMDMs

A & B) 1cM-PFAG had the highest bioactivity for limiting oxLDL uptake at an oxLDL concentration of 5 μg/mL ($n \geq 5$, * $p < 0.01$ compared to the following controls: ferulic acid, PSPEG-PFAG, PSPEG-PS, and 5 μg/mL oxLDL, ** $p < 0.05$ compared to 1cM-M12 for 5 μg/mL oxLDL). C) Representative fluorescent images of oxLDL (green) at at 5 μg/mL confirming flow cytometry results. Scale bar = 50 μm. D) Macrophages treated with1cM-PFAG maintain the lowest uptake of oxLDL at a concentration of 50 μg/mL ($n \geq 5$, # $p < 0.01$ compared to ferulic acid and 50 μg/mL oxLDL). E) Representative fluorescent images of cells treated with 50 μg/mL oxLDL (green) confirming flow cytometry results. Scale bar = 50 μm.

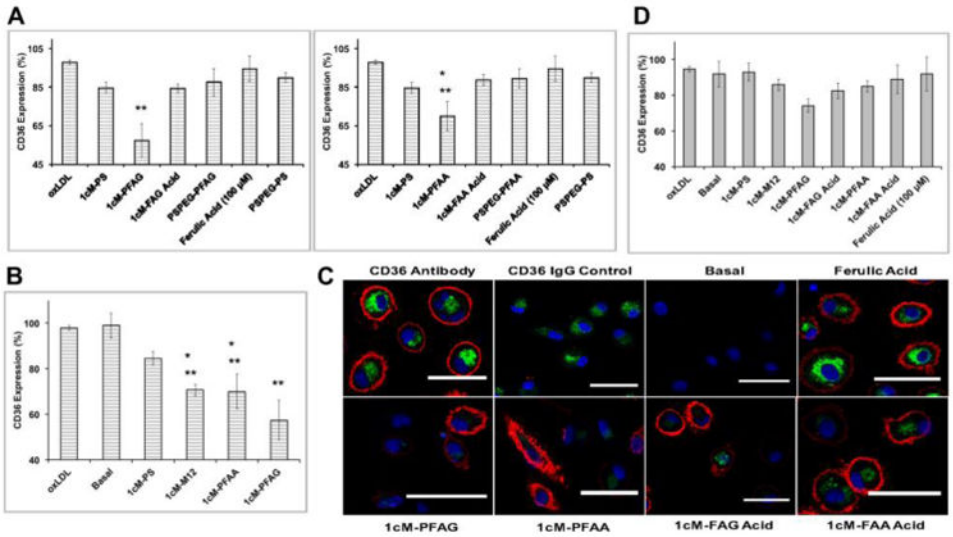

Figure 3. Composition of Ferulic Acid-based Poly(anhydride-ester) Nanoparticles differentially modulates CD36 expression in HMDMs

A-B) 1cM-PFAG down regulated CD36 expression by about 40% (oxLDL 5 μg/mL) ($n \geq 3$, ** $p < 0.01$ compared to 1cM-PS, 1cM-PFAG Acid, 1cM-PFAA Acid, ferulic acid, and oxLDL). 1cM-M12 and 1cM-PFAA also down regulated CD36 expression by about 30% (oxLDL 5 μg/mL) ($n \geq 3$, * $p < 0.05$ compared to ferulic acid, ** $p < 0.01$ compared to oxLDL). C). Representative fluorescent images of cells treated with 5 ug/ml oxLDL (green), Cell nuclei (blue), CD36 expression (red), which confirm flow cytometry results. Scale bar = 50 μm. D) CD36 expression increased for 1cM-M12, 1cM-PFAG, and 1cM-PFAA with increased oxLDL (50 μg/mL).

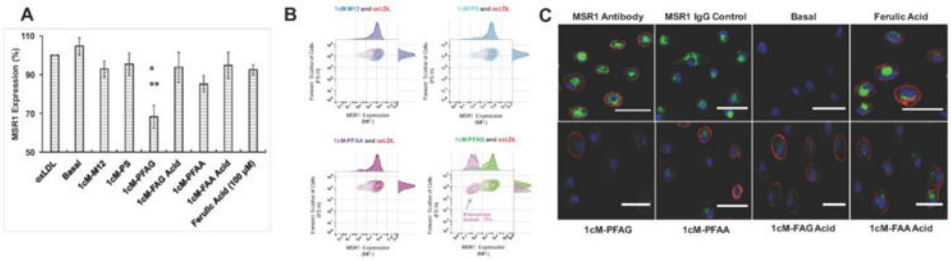

Figure 4. Composition of Ferulic Acid-based Poly(anhydride-ester) Nanoparticles differentially modulates MSR1 expression in HMDMs

A) 1cM-PFAG down regulated MSR1 expression by about 30% (oxLDL 5 μg/mL) (n = 3, * $p < 0.05$ compared to 1cM-PS, 1cM-PFAA Acid; ** $p < 0.01$ compared to oxLDL). B) Flow cytometry graphs are depicted as the forward scatter of cells (FS-H) versus 5 μg/mL oxLDL. A macrophage subset (5 ug/mL oxLDL) was observed with decreased MSR1 expression after treatment with 1cM-PFAG compared to 1cM-PFAA, 1cM-M12, and 1cM-PS. The size of this macrophage subset is slightly smaller than the entire population as evidenced by the small decrease in forward scatter of cells. expression in HMDMs. C) Representative fluorescent images of cells treated with 5 ug/ml oxLDL (green), cell nuclei (blue) and MSR1 expression (red), which confirm flow cytometry results. Scale bar = 50 μm.

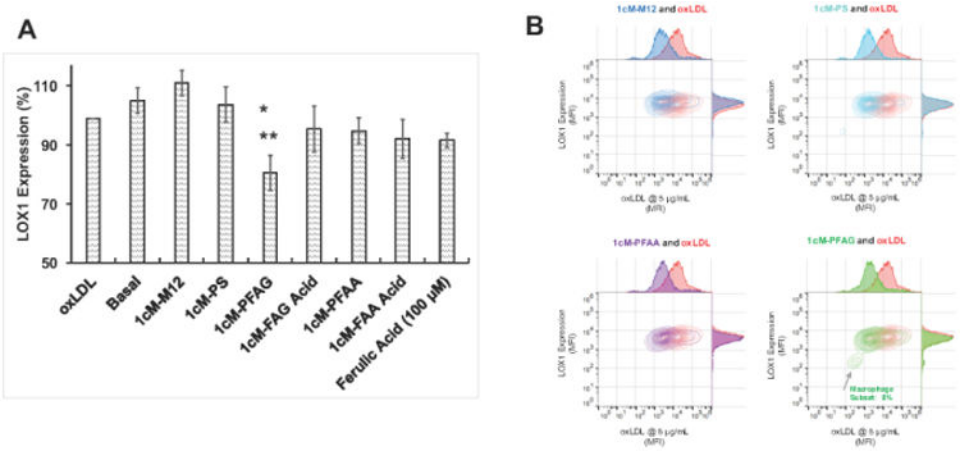

Figure 5. Composition of Ferulic Acid-based Poly(anhydride-ester) Nanoparticles differentially modulates LOX1 expression in HMDMs

A) 1cM-PFAG down regulated LOX1 expression by about 20% (oxLDL 5 μg/mL) (n ≥3, * $p < 0.05$ compared to 1cM-PS; ** $p < 0.01$ compared to 1cM-M12). B) Flow cytometry graphs are depicted as LOX-1 expression versus 5 μg/mL oxLDL. A macrophage subset (5 ug/mL oxLDL) was observed by with decreased LOX-1 expression after treatment with 1cM-PFAG compared to 1cM-PFAA, 1cM-M12, and 1cM-PS.

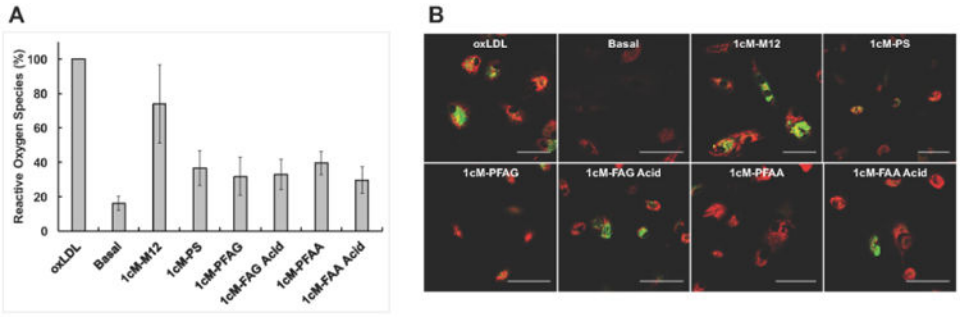

Figure 6. Effect of composition of Ferulic Acid-based Poly(anhydride-ester) Nanoparticles on reactive oxygen species (ROS) generation in HMDMs

A) Macrophages treated with 1cM-PFAG show the lowest levels of ROS generation compared to the oxLDL control at 50 μg/mL ($n = 4$, * $p < 0.05$ compared to oxLDL). B) Representative fluorescent images of oxLDL (green) at 50 μg/mL and ROS (red) show 1cM-PFAG has the highest potential to limit ROS generation. All scale bars represent 50 μm.